Relaxation dynamics in fluids of platelike colloidal particles

Markus Bier* and René van Roij
Institute for Theoretical Physics, Utrecht University, Leuvenlaan 4, 3584CE Utrecht, The Netherlands
(Received 1 May 2007; revised manuscript received 8 June 2007; published 29 August 2007)

The relaxation dynamics of a model fluid of platelike colloidal particles is investigated by means of a phenomenological dynamic density functional theory. The model fluid approximates the particles within the Zwanzig model of restricted orientations. The driving force for time dependence is expressed completely by gradients of the local chemical potential, which in turn is derived from a density functional—hydrodynamic interactions are not taken into account. These approximations are expected to lead to qualitatively reliable results for low densities like those within the isotropic-nematic two-phase region. The formalism is applied to model an initially spatially homogeneous stable or metastable isotropic fluid which is perturbed by switching a two-dimensional array of Gaussian laser beams. Switching on the laser beams leads to an accumulation of colloidal particles in the beam centers. If the initial chemical potential and the laser power are large enough, a preferred orientation of particles occurs, breaking the symmetry of the laser potential. After switching off the laser beams again, the system can follow different relaxation paths: It either relaxes back to the homogeneous isotropic state or it forms an approximately elliptical high-density core which is elongated perpendicular to the dominating orientation in order to minimize the surface free energy. For large supersaturations of the initial isotropic fluid, the high-density cores of neighboring laser beams of the two-dimensional array merge into complex superstructures.

DOI: 10.1103/PhysRevE.76.021405 PACS number(s): 83.80.Hj, 61.20.Lc, 64.60.My, 64.70.Md

I. INTRODUCTION

Fluids of platelike colloidal particles, e.g., clay suspensions, are of enormous fundamental and technological relevance because of their abundance and their distinct properties, due to the orientational degrees of freedom of the constituting particles. These systems exhibit many interesting phenomena such as flocculation, gelation, aging, and even liquid-crystal phase transitions [1–11]. During the last decade quite some progress has been made in both the synthesis [12,13] and the theoretical description of the equilibrium structure [14–25] of suspensions of platelike colloidal particles. However, understanding the *nonequilibrium* properties of these systems is still a big challenge.

Systems out of equilibrium are commonly analyzed either by investigating the relaxation of the system into equilibrium after an instant change of the conditions, e.g., due to switching an external field, or by studying the system in a (nonequilibrium) stationary state. The present theoretical work is devoted to the former case of relaxation within a model fluid of platelike colloidal particles; stationary states will be addressed in the future.

In view of the spatial inhomogeneities expected to be found, which in equilibrium systems are most adequately described by density functional theory (DFT) [26–28], the current investigation is performed within the framework of a phenomenological dynamic density functional theory (DDFT), which proposes an equation of motion for the particle number density profiles [29]. The latter are assumed to describe the state of the system completely, as within DFT any relevant quantity is a functional of the densities. Moreover, DFT is reproduced as the stationary limit of DDFT.

The motivation of the DDFT equation within this work follows the traditional reasoning known from treatments of time-dependent Landau-Ginzburg and Cahn-Hillard models in studies of critical dynamics, spinodal decomposition, and crystal growth [30–33]: the larger the thermodynamic distance from equilibrium, the faster the change of the state of the system. In the present case, the state can change due to translation as well as due to rotation of the platelike colloidal particles. Moreover, the total number of particles in the system is conserved, whereas the orientation is not. Hence the DDFT to be detailed in Sec. II is analogous to model C in the classification of Hohenberg and Halperin [34]. Alternatively, the present DDFT can be regarded as an elaborate phase field theory [35,36] with the order parameter tensor as the natural phase field.

In recent years, DDFT equations have been derived based on (overdamped) Langevin dynamics by approximating the time-dependent two-particle density [37–40]. As Langevin dynamics is considered a reasonable description for dilute colloidal suspensions, and as the isotropic-anisotropic liquid-crystal phase transitions in fluids of highly anisotropic colloidal particles take place at small number densities, DDFT is expected to be applicable within the isotropic-nematic two-phase region of fluids of platelike colloidal particles.

Here, relaxation dynamics is investigated by considering a two-step switching process: First an initially homogeneous stable or metastable isotropic state is brought out of equilibrium by switching on a two-dimensional array of Gaussian laser beams. The laser potential acts as an external potential which tends to form an inhomogeneous equilibrium state. In Sec. III, the relaxation toward this inhomogeneous equilibrium state is traced by integrating the DDFT equation for the presence of the laser potential. After equilibrating the system in the presence of a laser potential, the laser beams are switched off and the dynamics is described by the DDFT equation for vanishing external field. The system either re-

*m.bier@phys.uu.nl

laxes back to the initial isotropic state or evolves into an anisotropic state. The various relaxation paths will be analyzed in Sec. IV. This switching process has been chosen because it is expected to be realizable in experiments and, at the same time, numerically convenient boundary conditions can be used. As an illustration, and in order to allow for quantitative comparison, the model parameters have been chosen to describe an aqueous suspension of sterically stabilized gibbsite platelets [41].

Section V concludes the present work with a discussion of the applied formalism and the numerical results.

II. FORMALISM

A. Model fluid

The system under consideration is a colloidal suspension of monodisperse hard platelike particles dispersed within a continuous solvent. The colloidal particles are modeled by square cuboids which can take only one out of three mutually perpendicular orientations (Zwanzig approximation [42]), chosen to be parallel to the Cartesian axes. A particle is called an i particle if its square face normal points along the i axis, $i \in \{x,y,z\}$. The local number density of i particles at position $\mathbf{r}$ is denoted by $\varrho_i(\mathbf{r})$, and the abbreviation $\underline{\varrho} := (\varrho_x, \varrho_y, \varrho_z)$ is used for convenience. The structure of the model fluid is adequately described in terms of the total density $\varrho := \Sigma_i \varrho_i$ and the order parameter tensor Q [43] which, within Zwanzig models, is given by the diagonal form

$$Q_{ii'} = \frac{1}{2}\left(3\frac{\varrho_i}{\varrho} - 1\right)\delta_{ii'}. \tag{1}$$

Here $\delta_{ii'}$ denotes the Kronecker delta.

B. Equilibrium density functional theory

Density functional theory [26,27] is the method of choice in order to investigate equilibrium properties of spatially inhomogeneous fluids [28]. An accurate version of DFT for the Zwanzig model, which reproduces the exact second and third virial coefficients and which possesses the property of dimensional crossover, is the fundamental measure theory due to Cuesta and Martínez-Ratón [44,45]. It has been applied to investigate monodisperse [18,46] and polydisperse [47] Zwanzig models. Within this framework, the free energy functional is given by

$$\beta F[\underline{\varrho}] = \int d^3r \left(\sum_i \varrho_i(\mathbf{r})\{\ln[\varrho_i(\mathbf{r})\Lambda^3] - 1 + \beta V_i(\mathbf{r})\} + \Phi(\underline{n}(\mathbf{r})) \right), \tag{2}$$

where β is the inverse temperature, Λ denotes the thermal de Broglie wavelength, $V_i(\mathbf{r})$ represents the external potential exerted on i particles at position $\mathbf{r}$, and

$$\Phi(\underline{n}(\mathbf{r})) = n_0(\mathbf{r})\ln[1-n_3(\mathbf{r})] + \frac{\sum_q n_{1q}(\mathbf{r})n_{2q}(\mathbf{r})}{1-n_3(\mathbf{r})} + \frac{\prod_q n_{2q}(\mathbf{r})}{[1-n_3(\mathbf{r})]^2} \tag{3}$$

describes the local excess free energy density. The latter is a function of the weighted densities $n_\alpha(\mathbf{r}) := \Sigma_i \omega_{\alpha,i} \otimes \varrho_i(\mathbf{r})$ with $\otimes$ denoting convolution and weight functions defined by

$$\begin{aligned}
\omega_{0,i}(\mathbf{r}) &= a(r_x,S_{xi})a(r_y,S_{yi})a(r_z,S_{zi}),\\
\omega_{1x,i}(\mathbf{r}) &= b(r_x,S_{xi})a(r_y,S_{yi})a(r_z,S_{zi}),\\
\omega_{1y,i}(\mathbf{r}) &= a(r_x,S_{xi})b(r_y,S_{yi})a(r_z,S_{zi}),\\
\omega_{1z,i}(\mathbf{r}) &= a(r_x,S_{xi})a(r_y,S_{yi})b(r_z,S_{zi}),\\
\omega_{2x,i}(\mathbf{r}) &= a(r_x,S_{xi})b(r_y,S_{yi})b(r_z,S_{zi}),\\
\omega_{2y,i}(\mathbf{r}) &= b(r_x,S_{xi})a(r_y,S_{yi})b(r_z,S_{zi}),\\
\omega_{2z,i}(\mathbf{r}) &= b(r_x,S_{xi})b(r_y,S_{yi})a(r_z,S_{zi}),\\
\omega_{3,i}(\mathbf{r}) &= b(r_x,S_{xi})b(r_y,S_{yi})b(r_z,S_{zi}),
\end{aligned} \tag{4}$$

where the abbreviations $a(r,S) := \frac{1}{2}[\delta(S/2+r)+\delta(S/2-r)]$ and $b(r,S) := \Theta(S/2-|r|)$ are used, and S_{qi} denotes the extension of i particles along the q axis. The term "fundamental measure theory" is related to the geometric interpretation of spatial integrals of the weight functions of Eq. (4) as particle number, linear extension in the x, y, and z directions, cross-sectional area perpendicular to the x, y, and z axes, and particle volume, respectively.

Within a canonical system the equilibrium density profiles $\underline{\varrho}^{\mathrm{eq}}$ minimize $F[\underline{\varrho}]$ under the constraint

$$\int d^3r \sum_i \varrho_i(\mathbf{r}) = \text{const}. \tag{5}$$

The corresponding Lagrange multiplier is the chemical potential μ. With the local chemical potential

$$\mu_i(\mathbf{r},[\underline{\varrho}]) := \left.\frac{\delta F}{\delta \varrho_i(\mathbf{r})}\right|_{\underline{\varrho}}, \tag{6}$$

$\underline{\varrho}^{\mathrm{eq}}$ satisfies the Euler-Lagrange equation

$$\mu_i(\mathbf{r},[\underline{\varrho}^{\mathrm{eq}}]) = \mu, \tag{7}$$

i.e., equilibrium density profiles render the local chemical potential as a function of position ($\mathbf{r}$) and orientation (i) into a constant.

C. Dynamic density functional theory

A system initially out of equilibrium will be driven toward equilibrium. Motivated by equilibrium DFT, it will be assumed that the state of the system is described by time-dependent density profiles $\underline{\varrho}(\cdot,t)$. This assumption implies

neglect of hydrodynamic interactions, which depend on the velocity field. It is found that hydrodynamic interactions become more and more relevant for increasing packing fractions [48,49]. As the proposed theory is intended to be applied to dilute colloidal suspensions, not taking hydrodynamic interactions into account is considered to be a reasonable approximation.

In order to investigate the temporal evolution of the system, an equation of motion for $\underline{\varrho}(\cdot,t)$ has to be prescribed. Here the following form is proposed:

$$\frac{\partial \varrho_i(\mathbf{r},t)}{\partial t} = \left(\frac{\partial \varrho_i(\mathbf{r},t)}{\partial t}\right)_{\text{trans}} + \left(\frac{\partial \varrho_i(\mathbf{r},t)}{\partial t}\right)_{\text{rot}}, \tag{8}$$

where the first term on the right-hand side describes the contribution due to the translation of particles with fixed orientation, and the second term represents the contribution due to the rotation of particles keeping the local total density $\varrho(\mathbf{r},t)$ constant.

The translational part satisfies the continuity equation

$$\left(\frac{\partial \varrho_i(\mathbf{r},t)}{\partial t}\right)_{\text{trans}} := -\sum_q \frac{\partial j_{iq}(\mathbf{r},[\underline{\varrho}(\cdot,t)])}{\partial r_q}, \tag{9}$$

where j_{iq} describes the translational current of the i particles in the q direction. Following Dieterich *et al.* [29], the current is assumed to be proportional to the local density and to the negative gradient of the local chemical potential:

$$j_{iq}(\mathbf{r},[\underline{\varrho}(\cdot,t)]) := -\Gamma_{iq}\varrho_i(\mathbf{r},t)\frac{\partial \beta\mu_i(\mathbf{r},[\underline{\varrho}(\cdot,t)])}{\partial r_q}. \tag{10}$$

Here the *translational diffusion matrix* Γ with

$$\Gamma_{iq} = \begin{cases} \Gamma_{\parallel}, & i = q, \\ \Gamma_{\perp}, & i \neq q \end{cases} \tag{11}$$

accounts for different diffusivity of platelike colloidal particles parallel ($\Gamma_{\parallel}$) and perpendicular ($\Gamma_{\perp}$) to the symmetry axis.

The rotational part of Eq. (8) is modeled by a master equation

$$\left(\frac{\partial \varrho_i(\mathbf{r},t)}{\partial t}\right)_{\text{rot}} = \left(\frac{\partial \varrho_i(\mathbf{r},t)}{\partial t}\right)_{\text{rot}}^{\text{gain}} + \left(\frac{\partial \varrho_i(\mathbf{r},t)}{\partial t}\right)_{\text{rot}}^{\text{loss}}, \tag{12}$$

with the "gain" term

$$\left(\frac{\partial \varrho_i(\mathbf{r},t)}{\partial t}\right)_{\text{rot}}^{\text{gain}} \sim \sum_{i'} \{\beta\mu_{i'}(\mathbf{r},[\underline{\varrho}(\cdot,t)]) - \beta\mu_i(\mathbf{r},[\underline{\varrho}(\cdot,t)])\}\varrho_{i'}(\mathbf{r},t) \tag{13}$$

and the "loss" term

$$\left(\frac{\partial \varrho_i(\mathbf{r},t)}{\partial t}\right)_{\text{rot}}^{\text{loss}} \sim -\sum_{i'} \{\beta\mu_i(\mathbf{r},[\underline{\varrho}(\cdot,t)]) - \beta\mu_{i'}(\mathbf{r},[\underline{\varrho}(\cdot,t)])\}\varrho_i(\mathbf{r},t). \tag{14}$$

Hence

$$\left(\frac{\partial \varrho_i(\mathbf{r},t)}{\partial t}\right)_{\text{rot}} := -\frac{1}{6\tau}\sum_{i'} [\varrho_i(\mathbf{r},t) + \varrho_{i'}(\mathbf{r},t)]\{\beta\mu_i(\mathbf{r},[\underline{\varrho}(\cdot,t)]) - \beta\mu_{i'}(\mathbf{r},[\underline{\varrho}(\cdot,t)])\}. \tag{15}$$

The proportionality factors of Eqs. (13) and (14) equal the rotational diffusion coefficient, which in terms of the rotational relaxation time τ is given by $1/6\tau$.

In the limit of infinitely thin platelike colloidal particles, Brenner [50] has worked out translational and rotational diffusion coefficients. These expressions in the present notation lead to the rotational relaxation time

$$\tau = \frac{2}{9}\beta\eta D^3, \tag{16}$$

where η is the viscosity of the solvent and D denotes the diameter of the platelike colloidal particles, and to

$$\Gamma_{\parallel}\tau = \frac{D^2}{36}, \quad \Gamma_{\perp}\tau = \frac{D^2}{24}. \tag{17}$$

Equations (8)–(10) and (15) together with the definition Eq. (6) and the density functional Eqs. (2)–(4) completely specify the dynamic density functional theory for the Zwanzig particles to be investigated within this work.

Integration of the equation of motion Eq. (8) with an initial configuration $\underline{\varrho}(\cdot,0)$ leads to the time-dependent density profile $\underline{\varrho}$, which contains all spatial and temporal information.

The proposed DDFT is consistent with equilibrium DFT as any equilibrium state $\underline{\varrho}^{\text{eq}}$ satisfies Eq. (7) and therefore does not change under the dynamics represented by Eqs. (8)–(10) and (15).

D. External potential

Section III studies the relaxation of the model fluid within an external field. In view of conceivable experimental realizations this potential is chosen to model a two-dimensional array of Gaussian laser beams. Following the notation of Ref. [51], the force density on an inhomogeneous dielectric fluid is given by

$$\mathbf{f}(\mathbf{r}) = -\frac{1}{2}\varepsilon_0\overline{\mathbf{E}^2}(\mathbf{r})\,\boldsymbol{\nabla}\,\varepsilon(\mathbf{r}), \tag{18}$$

where ε_0 is the permeability of the vacuum, $\overline{\mathbf{E}^2}$ denotes the temporally averaged square of the local electric field, and $\varepsilon(\mathbf{r})$ is the local relative permeability. A single Gaussian beam of width w and power P propagating parallel to the z axis is described by [51]

$$\overline{\mathbf{E}^2}(\mathbf{r}) = \frac{2P}{\pi n\varepsilon_0 c w^2}\exp\left(-\frac{2(r_x^2 + r_y^2)}{w^2}\right) \tag{19}$$

with the refractive index n and the speed of light c. The total force $\mathbf{F}_i(\mathbf{r})$ exerted on a single i particle at position $\mathbf{r}$ is given by an integration of $\mathbf{f}$ over the particle volume. Given the refractive indices of the solvent, n_{solv}, and of the colloidal

particle, n_{coll}, ε can be assumed to change discontinuously from n_{solv}^2 outside the particle to n_{coll}^2 inside the particle. The aforementioned volume integration hence reduces to a surface integration, which can readily be performed in the case of Zwanzig particles. It is found that $\mathbf{F}_i(\mathbf{r})=-\boldsymbol{\nabla}V_i(\mathbf{r})$ with the laser potential of a single beam

$$V_i(\mathbf{r}) = -\frac{P(n_{\mathrm{coll}}-n_{\mathrm{solv}})S_{zi}}{4c}u(r_x,S_{xi})u(r_y,S_{yi}), \qquad (20)$$

where S_{qi} denotes again the extension of i particles along the q axis and

$$u(r,S) := \mathrm{erf}\left[\frac{\sqrt{2}}{w}\left(r+\frac{S}{2}\right)\right] - \mathrm{erf}\left[\frac{\sqrt{2}}{w}\left(r-\frac{S}{2}\right)\right]. \qquad (21)$$

For $n_{\mathrm{coll}}>n_{\mathrm{solv}}$, the laser potential is attractive.

E. Choice of parameters and numerical method

In order to obtain solutions of the DDFT equation specified in Sec. II C, one has to fix the model parameters describing the particle geometry, the particle diffusivity, and the laser potential. In the following, these parameters have been arbitrarily chosen to model the aqueous suspension (viscosity $\eta=8.9\times10^{-4}$ Pa s, refractive index $n_{\mathrm{solv}}=1.33$) of sterically stabilized gibbsite platelets (refractive index $n_{\mathrm{coll}}=1.58$) sample A10P of Ref. [41] (diameter $D=165$ nm, aspect ratio 12) irradiated by a two-dimensional square array of laser beams each of power $P=10$ mW and width $w=5D$ propagating in the z direction. Neighboring laser beams within the two-dimensional array are chosen to be $30D$ apart.

Due to the periodicity of the total laser potential, the actually infinite system is described in terms of a finite system with periodic boundary conditions under the influence of one single laser beam centered at the origin. The density profiles, which vary only in the x and y directions but not in the z direction, are defined on a square of side length $30D$ with periodic boundaries. Due to symmetries of the external potential, only one-quarter has actually to be coded, which is done by means of a grid with spacing $D/2$. This grid leads to slightly broadened isotropic-nematic interfaces as compared to calculations with finer grids. However, such a minute inaccuracy is considered irrelevant as compared to the numerical advantage gained by the relatively coarse grid. A particularly efficient numerical implementation is possible if one approximates the colloidal particles by infinitely thin platelets; an exception is Eq. (20) where a thickness of $D/12$ is used in order to avoid a vanishing laser potential.

Figure 1 displays the orientationally averaged laser potential $\bar{V}:=\frac{1}{3}\Sigma_i V_i$ as well as the local difference V_x-V_y of the potentials exerted on the x and y particles. The attractive laser potential is approximately axially symmetric on the energy scale β^{-1} [Fig. 1(a)], whereas there are deviations on the energy scale $10^{-3}\beta^{-1}$ [Fig. 1(b)].

According to Eq. (16), the rotational relaxation time is given by $\tau\approx214$ μs. The calculated translational diffusion coefficients [see Eq. (17)] compare well with the measured ones of Ref. [41]. The DDFT equation is integrated with respect to time by means of the Euler-forward method with integration time steps of $\tau/100$.

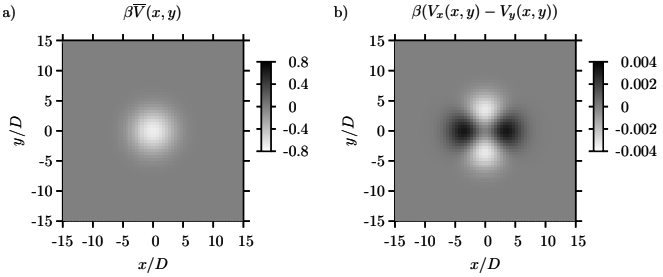

FIG. 1. (a) Orientationally averaged laser potential $\bar{V}(x,y)$ exhibiting an approximately axial symmetric attraction of platelike colloidal particles by the laser beam. (b) Deviations from the rotational symmetry appear on a smaller energy scale.

For the given set of parameters, one finds a first-order isotropic-nematic bulk phase transition at a reduced chemical potential $\mu_{\mathrm{b}}^*=-1.372\,716\,808\,465\,13$ with $\mu^* := \beta\mu-3\ln(2\Lambda/D)$. At this binodal (b) the isotropic bulk phase of density $\varrho_{\mathrm{b}}^{\mathrm{iso}}D^3\approx1.144$ coexists with the nematic bulk phase of density $\varrho_{\mathrm{b}}^{\mathrm{nem}}D^3\approx1.576$ and scalar order parameter $S=\langle\frac{3}{2}\cos(\vartheta)^2-\frac{1}{2}\rangle\approx0.83$, where $\langle\cdot\rangle$ denotes the thermal average and ϑ is the angle between the particle normal and the nematic director [43]. For illustrative purposes, the reduced chemical potentials μ^* are also expressed in terms of the supersaturation $\sigma:=(\varrho-\varrho_{\mathrm{b}}^{\mathrm{iso}})/\varrho_{\mathrm{b}}^{\mathrm{iso}}$ of an isotropic fluid of reduced chemical potential μ^*. The isotropic-nematic interfacial tensions for the nematic director pointing parallel and perpendicular to the interface normal are given by $\beta\gamma_{\parallel}D^2=2.051\,633\,048\times10^{-4}$ and $\beta\gamma_{\perp}D^2=3.832\,557\,464\times10^{-4}$, respectively. The isotropic spinodal (is) is located at the reduced chemical potential $\mu_{\mathrm{is}}^*\approx-1.128$, where the metastable isotropic state takes a density of $\varrho_{\mathrm{is}}^{\mathrm{iso}}D^3\approx1.244$. The nematic spinodal (ns) is located at the reduced chemical potential $\mu_{\mathrm{ns}}^*\approx-1.399$ where the stable isotropic state takes a density of $\varrho_{\mathrm{ns}}^{\mathrm{iso}}D^3\approx1.133$.

III. RELAXATION IN EXTERNAL FIELD

This section describes the influence of the external laser potential $V_j(\mathbf{r})$ (see Sec. II D) on an initially homogeneous isotropic fluid of platelike colloidal particles (see Sec. II A). Depending on the initial chemical potential, two qualitatively different scenarios are possible.

For reduced chemical potentials $\mu^*<\tilde{\mu}^*$, the fluid stays isotropic throughout and the laser potential merely leads to an axial symmetric accumulation of colloidal particles near the origin. For the parameters of Sec. II E, the limiting reduced chemical potential is $\tilde{\mu}^*\approx-1.6$ (supersaturation $\sigma\approx-0.080$).

However, if the initial reduced chemical potential satisfies $\mu^*>\tilde{\mu}^*$, the initial isotropic symmetry of the fluid is broken. Initially homogeneous states within the range $\mu^*\in(\tilde{\mu}^*,\mu_{\mathrm{is}}^*)$ exhibit the same qualitative behavior. Hence it is sufficient to describe the case of one initial state corresponding to, e.g., $\mu^*=-1.25$ ($\sigma=0.044$). A representation of the solutions of the DDFT equation in terms of the total density profile ϱ and the order parameter tensor component profiles Q_{xx} and Q_{yy} is displayed in Fig. 2.

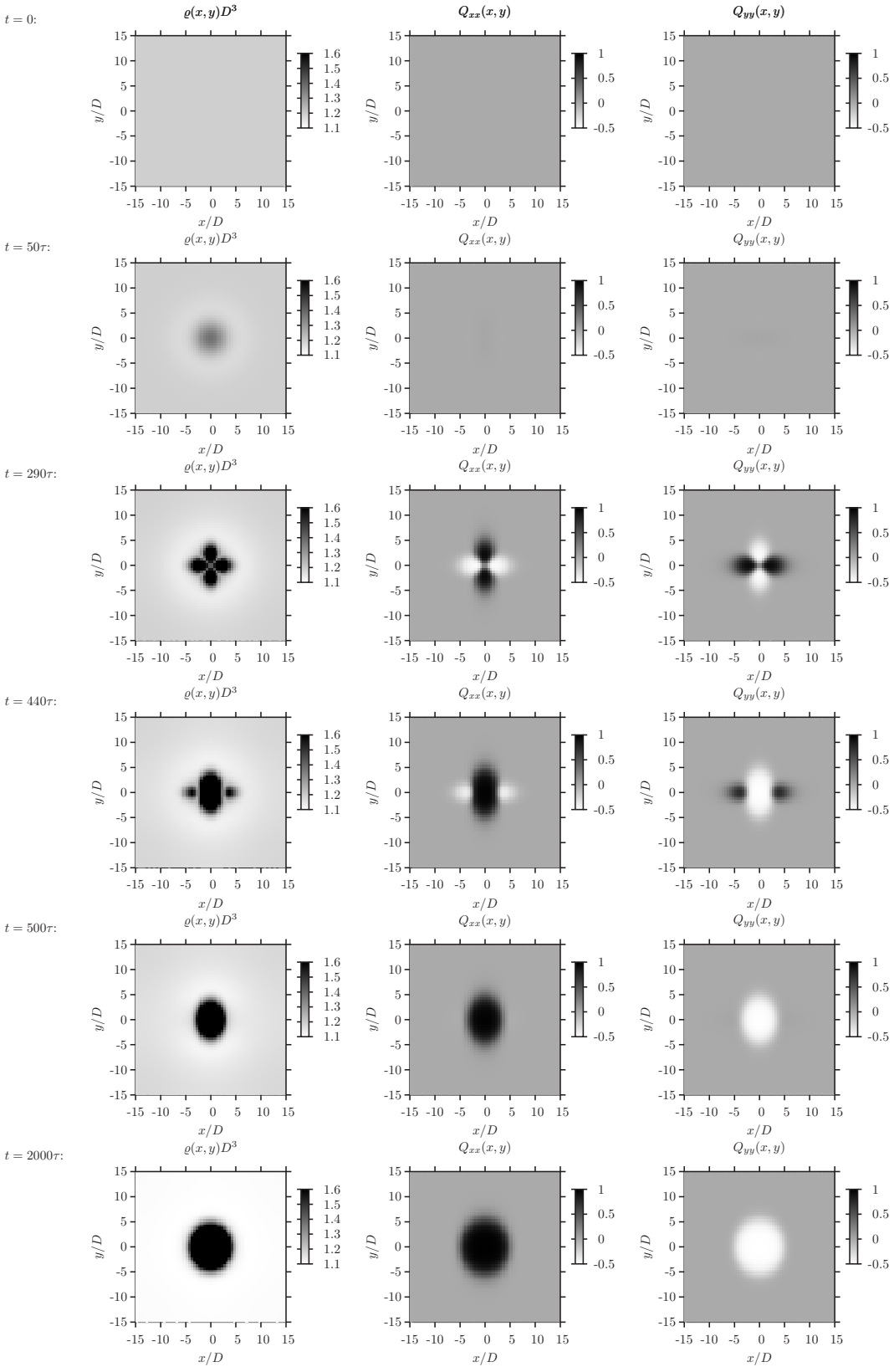

FIG. 2. Temporal evolution of an initially homogeneous supersaturated isotropic fluid of platelike colloidal particles under the influence of a laser potential in terms of the total density profile ϱ and the order parameter tensor component profiles Q_{xx} and Q_{yy}. The length scale D and the time scale τ correspond to the diameter and the rotational relaxation time of the colloidal particles, respectively. The equilibrium densities at isotropic-nematic two-phase coexistence are given by $\varrho_b^{iso}D^3 \approx 1.144$ for the isotropic state and $\varrho_b^{nem}D^3 \approx 1.576$ for the nematic state.

After a time of $t=50\tau$, slight distortions of the initial homogeneity due to the attraction of the colloidal particles by the laser beam become visible in the total density profile ϱ; the density at the origin is $\varrho(0,0)D^3\approx 1.382$. Orientational ordering, however, is still negligible.

At time $t=290\tau$, more particles have been concentrated near the origin $[\varrho(0,0)D^3\approx 1.450]$ at the expense of the direct surroundings. Moreover, four maxima of the total density profile ϱ formed near the origin $[\varrho(\pm 1.5D,0)D^3 = \varrho(0,\pm 1.5D)D^3\approx 2.250]$. The cubic symmetry of the total density profile ϱ and the rectangular symmetry of the order parameter components Q_{xx} and Q_{yy} reflect the orientation dependence of the external laser potential Eq. (20) [see Fig. 1(b)].

At $t=440\tau$, the cubic symmetry of the total density profile is broken by forming a bridge between two opposite peaks present at time $t=290\tau$. The density at the origin has increased to $\varrho(0,0)D^3\approx 2.723$. In the current case this bridge is formed by x particles, but a bridge made of y particles is possible as well. It has been confirmed that minute rounding-off errors in the very first integration step give rise to the formation of bridges of one or the other orientation. The two peaks of y particles, which do not form a bridge, have moved away from the origin, and the local maximum of the total density is given by $\varrho(\pm 3.5D,0)D^3\approx 1.648$. They are subsequently decreased because the nearby bridge forces the particles to take the x orientation and afterward join the bridge.

At time $t=500\tau$, the two peaks of y particles have disappeared completely. The approximately elliptical core (semiaxes of half height contour approximately $2.1D$ and $2.6D$) of increased particle concentration near the center $[\varrho(0,0)D^3 \approx 2.805]$ comprises mostly x particles. In the following, more and more particles from the surroundings are added to the high-density core, giving rise to a decrease of the total density outside the laser beam.

From time $t=2000\tau$ onward, the system is almost equilibrated and the state practically no longer changes in time. The final high-density core has, as the orientationally averaged laser potential $\bar{V}$ [Fig. 2(a)], an almost circular cross section (radius of half height contour approximately $2.9D$). The total density at the origin is $\varrho(0,0)D^3\approx 3.530$, whereas the minimum of approximately 1.101 is found at a distance of about $8.5D$ from the origin. Due to the small finite size (diameter $30D$) of the considered part of the total system, the total density at the (periodic) boundaries has been decreased to a value of $\varrho|_\partial D^3\approx 1.104$.

The trajectory of the system for $\mu^*>\tilde{\mu}^*$ can be summarized as follows. The laser potential, which is not axially symmetric (see Fig. 1), attracts particles to the origin and thereby creates four nematic nuclei (two of x particles and two of y particles), which compete at the origin. If one pair of nuclei breaks the symmetry at the origin, it forms a bridge, whereas the other pair of nuclei decays. This scenario hinges on the creation of the nematic nuclei and hence on a sufficiently strong laser potential: The limiting reduced chemical potential $\tilde{\mu}^*$ is expected to decrease upon increasing the laser power P. In particular, for sufficiently strong laser potentials, $\tilde{\mu}^*$ can be located well within the isotropic phase of the bulk phase diagram; i.e., the symmetry breaking scenario can occur for initial states that correspond to a stable isotropic fluid.

For a given initial reduced chemical potential μ^*, one can define a limiting laser power $\tilde{P}(\mu^*)$ such that the symmetry breaking scenario will take place if and only if $P>\tilde{P}(\mu^*)$. For the case $\mu^*=-1.25$ ($\sigma=0.044$) and the parameters of Sec. II E, the limiting laser power has been determined approximately as $\tilde{P}(-1.25)\approx 3.5$ mW.

IV. RELAXATION OF THE FREE FLUID

The previous section described the equilibration path of an initially homogeneous isotropic fluid within a laser potential. The equilibrium structure in the presence of the laser potential was attained after about $t=2000\tau$ (see Fig. 2). The present section is concerned with the temporal evolution of the fluid after switching off the laser beam at time $t^* := 2000\tau$. Three possible scenarios for the evolution of the free fluid have been identified, determined by the total density of the initial homogeneous isotropic fluid at time $t=0$.

If the total density at time $t=0$ is small ($\mu^*\lessapprox -1.32$, $\sigma\lessapprox 0.019$), the high-density core present at $t=t^*$ (see Sec. III) dissolves completely for $t\to\infty$ by releasing the excess amount of particles to the surroundings. Under these conditions the system relaxes back to the initial homogeneous isotropic state. In the case of a supersaturated initial isotropic system [$\mu^*\in(\mu_b^*,-1.32)$, $\sigma\in(0,0.019)$; see Sec. II E], classical nucleation theory would consider the perturbation due to the external potential too small to cross the high free energy barrier between the weakly supersaturated metastable isotropic state and a stable nematic state.

For intermediate initial supersaturation, the high-density core reshapes with time, attaining for $t\to\infty$ a finitely elongated, approximately elliptical shape. Figure 3 displays the structures of the almost equilibrated fluids for initial reduced chemical potentials $\mu^*\in\{-1.31,-1.27,-1.21\}$ (supersaturations $\sigma\in\{0.022,0.037,0.058\}$) at time $t=t^*+10\,000\tau$. These structures exhibit the same total density at the origin $\varrho(0,0)D^3\approx 1.62$, the same total density far from the origin $\varrho|_\partial D^3\approx 1.15$, as well as the same aspect ratio 1.85 of the half height contour. Note that the core extension of the equilibrium state can be as small as a few particle diameters [see the case $\mu^*=-1.31$ ($\sigma=0.022$) in Fig. 3]. Moreover, the high-density core imposes orientational order to such a degree that a preferred alignment of the platelike particles is found even within the dilution zone surrounding it.

An estimate of the aspect ratio of the equilibrium half height contour can be obtained within a sharp-kink approximation, which describes the equilibrium structures of Fig. 3 by a nematic ellipse surrounded by isotropic fluid where the isotropic-nematic interface is described by a step function. Assuming an angle-dependent interfacial tension $\gamma(\vartheta) := \gamma_\parallel\cos(\vartheta)^2+\gamma_\perp\sin(\vartheta)^2$, where ϑ denotes the angle between the contour normal and the nematic director, and where $\gamma_\parallel$ and $\gamma_\perp$ are the isotropic-nematic interfacial tensions given in Sec. II E, one obtains an approximate surface free energy $\tilde{F}_{\text{surf}}$ by integration of γ along the contour of an ellipse. Minimizing $\tilde{F}_{\text{surf}}$ with respect to the semiaxes of the

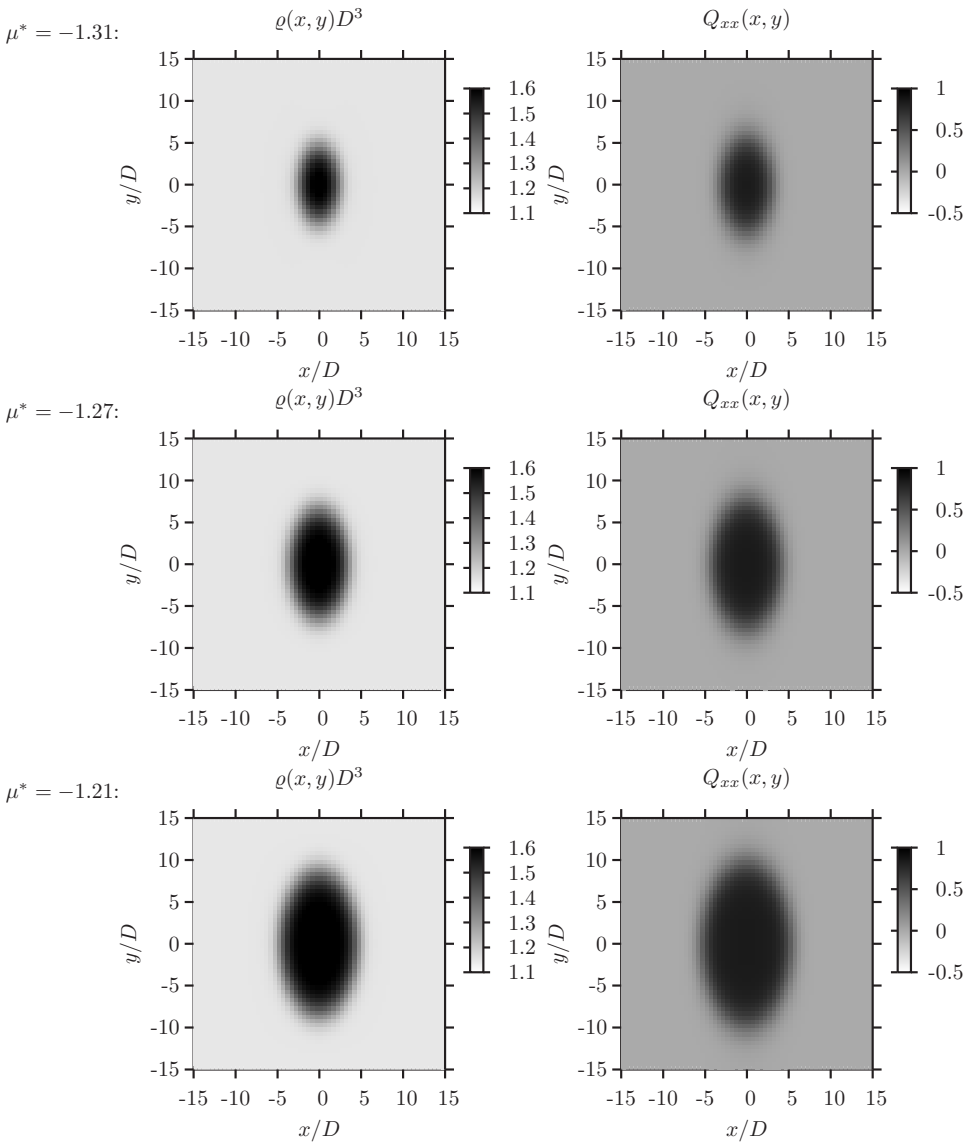

FIG. 3. Structure of a free fluid of platelike colloidal particles for reduced chemical potentials $\mu^* \in \{-1.31, -1.27, -1.21\}$ (supersaturations $\sigma \in \{0.022, 0.037, 0.058\}$) at time $t = t^* + 10\,000\tau$. The fluid has been exposed for a time interval $t^* = 2000\tau$ to a laser potential (see Fig. 2), which afterward was switched off. These structures represent the equilibrium structures as they no longer change in time.

ellipse under the constraint of constant area of the ellipse leads to the aspect ratio 1.842 49. This value agrees well with the value 1.85 of the equilibrium structures of Fig. 3. The calculation also shows that the aspect ratio depends only on the ratio of the interfacial tensions but not on the area of the ellipse.

Within the terminology of classical nucleation theory, the perturbation due to the laser potential has been large enough to cross the free energy barrier between the metastable isotropic state and a state containing an approximately elliptical nematic core surrounded by an isotropic fluid. In compliance with classical nucleation theory, the shape of the core is determined by a minimum of the surface free energy, and the densities within and outside the core are approximately given by the isotropic-nematic coexistence values. However, whereas classical nucleation theory and its generalizations [52] seek for the fluctuation-induced critical nucleus, which corresponds to the free energy "saddle point" between the metastable and stable states, the perturbations considered in the present work are of external origin and the free energy barrier is crossed along "higher" paths.

If the initial reduced chemical potential μ^* is sufficiently large, the high-density core contains enough particles to grow to the (periodic) boundary of the modeled part of the system, where it merges with its "images" into a system-spanning superstructure. Figure 4 displays this behavior for the case $\mu^* = -1.13$ ($\sigma = 0.087$). Directly after switching off the laser beams at time $t = t^*$, a circular high-density core with total density $\varrho(0,0)D^3 \approx 3.734$ is present. At time $t = t^* + 10\,000\tau$ the total density at the origin has decayed to $\varrho(0,0)D^3 \approx 1.62$ and the aspect ratio of the half height contour is 1.81. These values agree with those of the cases displayed in Fig. 3. However, the region of orientational order, which extends beyond the dense core, has reached the periodic boundaries of the system. The high-density core thereby interacts with its images, which leads to a further stretching as displayed for time $t = t^* + 15\,000\tau$. Finally the high-density core merges with its images, forming a bandlike structure with total densities $\varrho(0,0)D^3 \approx 1.58$ and $\varrho(\pm 15D, 0)D^3 \approx 1.14$. This structure corresponds to a lower free energy as compared to the approximately elliptical structure, because the isotropic-nematic interface is now everywhere parallel to

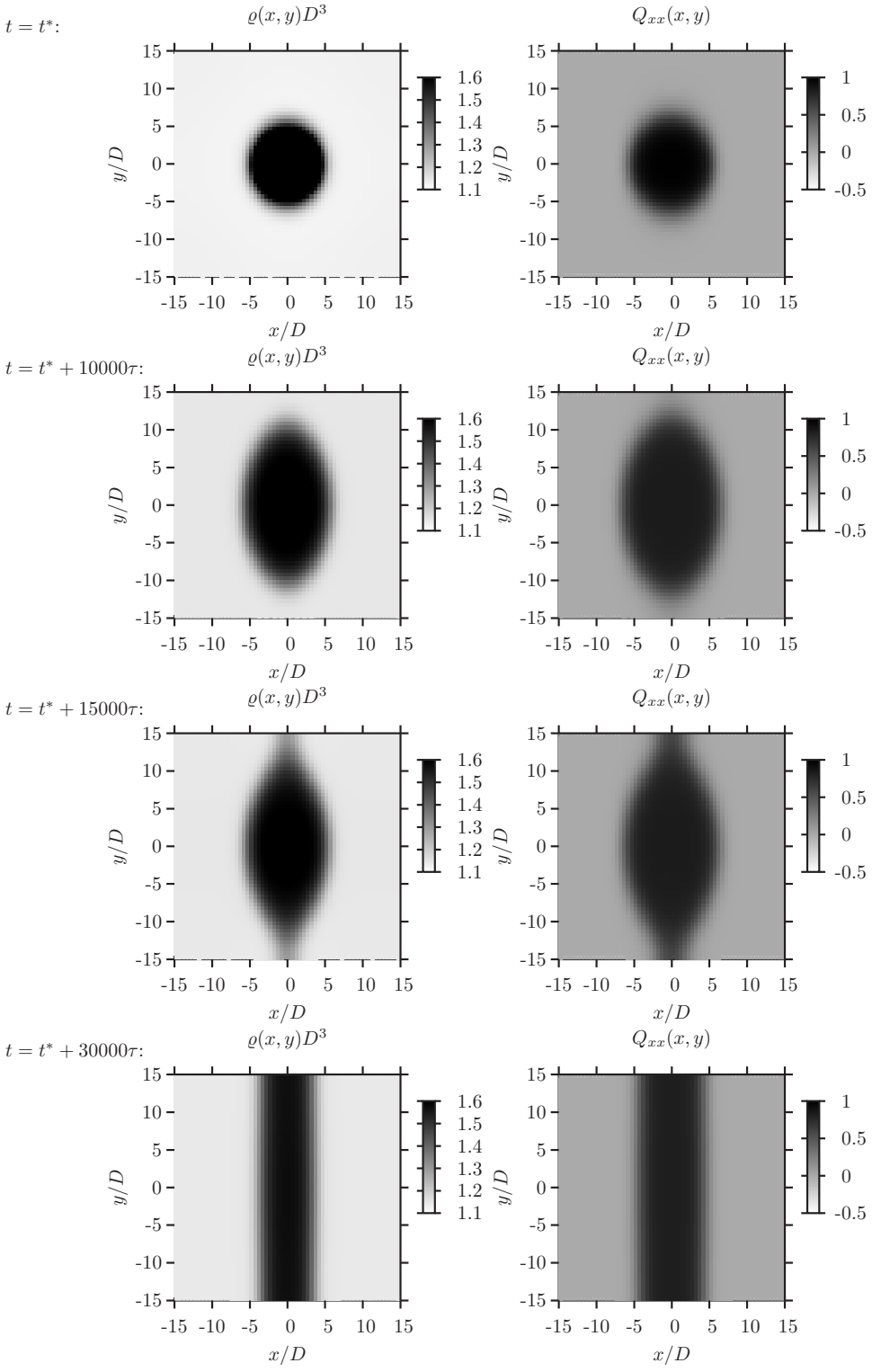

FIG. 4. Growth of the high-density core within a free fluid of platelike colloidal particles for initial reduced chemical potential $\mu^* = -1.13$ (supersaturation $\sigma = 0.087$). The fluid has been exposed for a time interval $t^* = 2000\tau$ to a laser potential (see Fig. 2), which afterward was switched off. The growing high-density core ultimately merges with its images due to periodic boundary conditions.

the nematic director. The time scale on which the high-density core stretches is much larger than the time scales of the processes observed in the presence of the laser potential (see Sec. III) because the chemical potential gradients and hence the currents are much smaller here. In an experimental realization, the high-density cores at the centers of the individual laser beams will be oriented in different directions. Upon merging the high-density cores, a complex networklike structure is expected to form.

V. DISCUSSION AND SUMMARY

The previous three sections introduced and applied a dynamic density functional theory for a model fluid of platelike colloidal particles. The particles are assumed to be infinitely thin, and the orientational degrees of freedom are taken approximately into account by restricting the particle normal to three mutually perpendicular directions (Zwanzig model [42]). Although qualitative, this model exhibits, in agreement

with experimental studies [9–11], an isotropic-nematic bulk phase transition at low number densities. Within the framework of DDFT, the state is described by a set of density profiles and the proposed equation of motion is constructed in order to fulfill the conservation of the total number of particles. Time dependence is generated by gradients of the local chemical potential, which is derived from a density functional. The phenomenological parameters appearing in the equation of motion are determined by matching the dilute limit with single-particle translational and rotational diffusion [50]. This approach does not take hydrodynamic interactions between colloidal particles into account, because they are assumed to be small for the small densities within the isotropic-nematic two-phase coexistence region considered here.

The proposed DDFT is applied to the investigation of relaxation dynamics of the model fluid. In a first step the relaxation of an initially homogeneous isotropic fluid in an external potential due to a two-dimensional array of laser beams (Fig. 1) is studied. The restriction on the orientational degrees of freedom of the particles leads to structures of rectangular symmetry (Fig. 2). In particular, a transient cubic symmetric total density profile changes into an only rectangular symmetric total density profile. For a model of continuous orientations, it can be expected to find an axial symmetry instead of the cubic symmetry. However, the spontaneous symmetry breaking into a rectangular symmetric equilibrium state is expected to be found for continuous orientational degrees of freedom, too.

For an infinite system initially prepared within the isotropic-nematic two-phase coexistence region and one single laser beam of sufficient strength, instead of an array of laser beams, one would expect an equilibrium structure composed of three regions: A narrow high-density core at the position of the laser beam is surrounded by an annulus of nematic structure of total density ϱ_b^{nem} (see Sec. II E) which is surrounded by an annulus of isotropic structure of total density ϱ_b^{iso} (see Sec. II E); the sizes of the isotropic and nematic annuli are related to the initial state by means of the "lever rule." In order to form this structure, the system has to be large enough such that the amount of fluid within the high-density core and the isotropic-nematic interface is negligible as compared to the total amount of fluid. However, the two-dimensional grid applied within this work does not allow for sufficiently large single-beam systems. In contrast, the smallness of the periodicity of the system considered in this work leads to a rather strong dilution of the fluid in the space between the laser beams.

In classical nucleation theory one considers the temporal evolution of fluctuation-induced "droplets" of the stable (nematic) phase surrounded by the metastable (isotropic) phase, where the densities are chosen as the two-phase coexistence values. The smallness of the periodicity of the current system, however, leads to a high-density core whose size equals the size of the laser beam and whose density is determined by the strength of the external potential. Therefore the high-density cores in this work are very different from the droplets considered in classical nucleation theory. Moreover, the relaxation paths here do not cross the "critical nucleus," which corresponds to the minimal perturbation that leads to the equilibrium state and which is located at a saddle point of the free energy [52]. Thus the current results can be partly looked at in terms of the terminology of classical nucleation theory, because both are based on a free energy function(al); however, the setup considered here is different from that of classical nucleation theory.

After attaining a state close to the equilibrium state in the presence of the laser potential, the laser beams are switched off and the relaxation of the (now) free fluid to equilibrium is traced. For sufficiently large initial supersaturation of the initial state, one finds the central region of increased particle density stretching (Fig. 3). The shape of these cores resembles tactoids which have been found in dispersions of rodlike colloidal particles [53]. If the moving density fronts hit the periodic boundaries of the modeled part of the system they merge with their images into a superstructure (Fig. 4). As the nematic directors within the high-density cores of the individual laser beams may point in different directions, the merging of two neighboring cores is expected to give rise to one more relaxation process in which the merging cores reorient their colloidal particles along a common nematic director. This effect, however, is beyond the present study.

In summary, a dynamic density functional theory for a model of fluids of platelike colloidal particles has been proposed and applied to the relaxation dynamics of the fluid under the influence of the potential of a two-dimensional array of laser beams. A rich phenomenology, including the occurrence of individual approximately elliptical high-density cores and the possible formation of complex superstructures, has been found.

ACKNOWLEDGMENTS

The authors like to thank Paul van der Schoot for helpful discussions and Marjolein Dijkstra for access to additional computational resources. This work is part of the research program of the "Stichting voor Fundamenteel Onderzoek der Materie (FOM)," which is financially supported by the "Nederlandse Organisatie voor Wetenschappelijk Onderzoek (NWO)."

[1] A. Mourchid, A. Delville, J. Lambard, E. Lécolier, and P. Levitz, Langmuir **11**, 1942 (1995).
[2] A. B. D. Brown, S. M. Clarke, and A. R. Rennie, Langmuir **14**, 3129 (1998).
[3] A. Mourchid, E. Lécolier, H. van Damme, and P. Levitz, Langmuir **14**, 4718 (1998).
[4] D. Bonn, H. Kellay, H. Tanaka, G. Wegdam, and J. Meunier, Langmuir **15**, 7534 (1999).
[5] A. B. D. Brown, C. Ferrero, T. Narayanan, and A. R. Rennie, Eur. Phys. J. B **11**, 481 (1999).

[6] P. Levitz, E. Lécolier, A. Mourchid, A. Delville, and S. Lyonnard, Europhys. Lett. **49**, 672 (2000).
[7] A. Knaebel, M. Bellour, M.-P. Munch, V. Viasnoff, F. Lequeux, and J. L. Harden, Europhys. Lett. **52**, 73 (2000).
[8] B. Abou, D. Bonn, and J. Meunier, Phys. Rev. E **64**, 021510 (2001).
[9] D. van der Beek and H. N. W. Lekkerkerker, Europhys. Lett. **61**, 702 (2003).
[10] D. van der Beek and H. N. W. Lekkerkerker, Langmuir **20**, 8582 (2004).
[11] N. Wang, S. Liu, J. Zhang, Z. Wu, J. Chen, and D. Sun, Soft Matter **1**, 428 (2005).
[12] F. M. van der Kooij and H. N. W. Lekkerkerker, J. Phys. Chem. B **102**, 7829 (1998).
[13] S. Liu, J. Zhang, N. Wang, W. Liu, C. Zhang, and D. Sun, Chem. Mater. **15**, 3240 (2003).
[14] J. A. Cuesta and R. P. Sear, Eur. Phys. J. B **8**, 233 (1999).
[15] D. G. Rowan and J.-P. Hansen, Langmuir **18**, 2063 (2002).
[16] L. Harnau, D. Costa, and J.-P. Harnau, Europhys. Lett. **53**, 729 (2001).
[17] L. Harnau and S. Dietrich, Phys. Rev. E **65**, 021505 (2002).
[18] L. Harnau, D. Rowan, and J.-P. Hansen, J. Chem. Phys. **117**, 11359 (2002).
[19] M. Bier, L. Harnau, and S. Dietrich, Phys. Rev. E **69**, 021506 (2004).
[20] L. Harnau and S. Dietrich, Phys. Rev. E **69**, 051501 (2004).
[21] D. Costa, J.-P. Hansen, and L. Harnau, Mol. Phys. **103**, 1917 (2005).
[22] L. Harnau and S. Dietrich, Phys. Rev. E **71**, 011504 (2005).
[23] L. Li, L. Harnau, S. Rosenfeldt, and M. Ballauff, Phys. Rev. E **72**, 051504 (2005).
[24] M. Bier, L. Harnau, and S. Dietrich, J. Chem. Phys. **123**, 114906 (2005).
[25] M. Bier, L. Harnau, and S. Dietrich, J. Chem. Phys. **125**, 184704 (2005).
[26] R. Evans, Adv. Phys. **28**, 143 (1979).
[27] R. Evans, in *Liquides aux Interfaces/Liquids at Interfaces*, edited by J. Charvolin, J. F. Joanny, and J. Zinn-Justin, Proceedings of the Les Houches Summer School of Theoretical Physics, XLVIII, 1988 (North-Holland, Amsterdam, 1989), p. 1.
[28] R. Evans, in *Inhomogeneous Fluids*, edited by D. Henderson (Marcel Dekker, New York, 1991), p. 89.
[29] W. Dieterich, H. L. Frisch, and A. Majhofer, Z. Phys. B: Condens. Matter **78**, 317 (1990).
[30] J. S. Langer, Ann. Phys. (N.Y.) **65**, 53 (1971).
[31] K. Kawasaki, Prog. Theor. Phys. **57**, 410 (1977).
[32] J. B. Collins and H. Levine, Phys. Rev. B **31**, 6119 (1985); **33**, 2020(E) (1986).
[33] P. R. Harrowell and D. W. Oxtoby, J. Chem. Phys. **86**, 2932 (1987).
[34] P. C. Hohenberg and B. I. Halperin, Rev. Mod. Phys. **49**, 435 (1977).
[35] W. J. Boettinger, J. A. Warren, C. Beckermann, and A. Karma, Annu. Rev. Mater. Res. **32**, 163 (2002).
[36] L. Gránásy, T. Pusztai, and T. Börzsönyi, in *Handbook of Theoretical and Computational Nanotechnology*, edited by M. Rieth and W. Schommers (American Scientific Publishers, Stevenson Ranch, California, i2006), Vol. 9, p. 525.
[37] D. S. Dean, J. Phys. A **29**, L613 (1996).
[38] U. M. B. Marconi and P. Tarazona, J. Chem. Phys. **110**, 8032 (1999).
[39] U. M. B. Marconi and P. Tarazona, J. Phys.: Condens. Matter **12**, A413 (2000).
[40] A. J. Archer and R. Evans, J. Chem. Phys. **121**, 4246 (2004).
[41] F. M. van der Kooij, A. P. Philipse, and J. K. G. Dhont, Langmuir **16**, 5317 (2000).
[42] R. Zwanzig, J. Chem. Phys. **39**, 1714 (1963).
[43] P. G. de Gennes and J. Prost, *The Physics of Liquid Crystals* (Oxford University Press, Oxford, 1993).
[44] J. A. Cuesta and Y. Martínez-Ratón, Phys. Rev. Lett. **78**, 3681 (1997).
[45] J. A. Cuesta and Y. Martínez-Ratón, J. Chem. Phys. **107**, 6379 (1997).
[46] Y. Martínez-Ratón and J. A. Cuesta, J. Chem. Phys. **111**, 317 (1999).
[47] Y. Martínez-Ratón and J. A. Cuesta, J. Chem. Phys. **118**, 10164 (2003).
[48] X. Qiu, X. L. Wu, J. Z. Xue, D. J. Pine, D. A. Weitz, and P. M. Chaikin, Phys. Rev. Lett. **65**, 516 (1990).
[49] J.-Z. Xue, X.-L. Wu, D. J. Pine, and P. M. Chaikin, Phys. Rev. A **45**, 989 (1992).
[50] H. Brenner, Int. J. Multiphase Flow **1**, 195 (1974).
[51] R. Gussard, T. Lindmo, and I. Brevik, J. Opt. Soc. Am. B **9**, 1922 (1992).
[52] D. W. Oxtoby and R. Evans, J. Chem. Phys. **89**, 7521 (1988).
[53] J. D. Bernal and I. Fankuchen, J. Gen. Physiol. **25**, 111 (1941).